SCIENTIFIC REPORTS

OPEN

SUBJECT AREAS:
BIOMATERIALS – PROTEINS
BIOMEDICAL MATERIALS
NANOBIOTECHNOLOGY
PROTEIN DELIVERY

Received
13 May 2013

Accepted
5 July 2013

Published
22 July 2013

Correspondence and requests for materials should be addressed to N.Y. (yui.org@tmd.ac.jp)

Molecular logistics using cytocleavable polyrotaxanes for the reactivation of enzymes delivered in living cells

Atsushi Tamura[1], Go Ikeda[1,2], Ji-Hun Seo[1], Koji Tsuchiya[2], Hirofumi Yajima[2], Yoshihiro Sasaki[1,3], Kazunari Akiyoshi[3] & Nobuhiko Yui[1]

[1]Department of Organic Biomaterials, Institute of Biomaterials and Bioengineering, Tokyo Medical and Dental University, 2-3-10 Kanda-Surugadai, Chiyoda, Tokyo 101-0062, Japan, [2]Department of Applied Chemistry, Faculty of Science, Tokyo University of Science, 1-3 Kagurazaka, Shinjuku, Tokyo 162-8601, Japan, [3]Department of Polymer Chemistry, Graduate School of Engineering, Kyoto University, A3-317 Katsura, Nishikyo, Kyoto 615-8510, Japan.

The intracellular delivery of enzymes is an essential methodology to extend their therapeutic application. Herein, we have developed dissociable supermolecule-enzyme polyelectrolyte complexes based on reduction-cleavable cationic polyrotaxanes (PRXs) for the reactivation of delivered enzymes. These PRXs are characterized by their supramolecular frameworks of a polymeric chain threading into cyclic molecules, which can form polyelectrolyte complexes with anionic enzymes while retaining their three dimensional structure, although their enzymatic activity is reduced. Upon the addition of a reductant, the PRXs dissociate into their constituent molecules and release the enzymes, resulting in a complete recovery of enzymatic activity. Under the intracellular environment, the PRX-based enzyme complexes showed the highest intracellular enzymatic activity and efficient activation of anticancer prodrugs to induce cytotoxic effects in comparison with the non-dissociable complexes and the commercial cell-penetrating peptide-based reagents. Thus, the intracellularly dissociable supermolecules are an attractive system for delivering therapeutic enzymes into living cells.

Protein therapeutics have received tremendous attention, and more than 100 protein therapeutics including antibodies, enzymes and peptides, are currently approved for clinical use[1,2]. Of these, enzymes are of significance in therapeutic approaches such as the enzyme replacement therapy and the enzyme-prodrug therapy[3,4]. Although these therapeutic approaches require cellular internalization of therapeutic enzymes, most of the enzymes have low ability to cross the cellular membrane, resulting in insufficient therapeutic efficacy[5]. To address this problem, cell-penetrating peptides (CPPs) are chemically or genetically linked to enzymes to improve *in vitro* and *in vivo* delivery[5–7]. Another promising approach for intracellular protein delivery is complex formation with polymeric materials or encapsulation in nanoparticles[8–11]. However, complex formation with polymers through electrostatic or hydrophobic interactions often causes a loss of the activity of the enzymes, most likely due to the mask of active site[12]. To regulate the enzymatic activity, various methodologies that can control the association and dissociation of the complexes have been achieved by using pH[13], electric fields[14], salt concentrations[15], the addition of polyelectrolytes[16,17], and other additives[18]. Although these methodologies are effective at regulating the enzymatic activity in response to physical or chemical stimuli to a certain extent, the potential of intracellular delivery and enzymatic control in intracellular environments is not yet known. Because the intracellular activity of enzymes plays a crucial role in enzyme-based therapy, strategies for molecular logistics are required to show efficient intracellular delivery as well as enhanced enzymatic activity in the intracellular environment.

We have developed a new modality of biodegradable supermolecules for the intracellular delivery and the subsequent release of biopharmaceuticals based on polyrotaxanes (PRXs)[19–21]. The PRXs consist of α-cyclodextrins (CDs) threaded along a poly(ethylene glycol) (PEG) chain and a terminal bulky stopper via intracellularly cleavable linkages such as disulfide linkages[21]. The supramolecular structure of cleavable PRXs is sufficiently stable under physiological conditions, whereas the PRXs degrade into their constituent molecules (*i.e.,* PEG and CD) when the terminal linkers are cleaved by intracellular stimuli. We have developed *N*,*N*-dimethylaminoethyl (DMAE) group-modified PRXs with terminal disulfide linkages (DMAE-SS-PRXs) as carriers for the intracellular delivery of plasmid DNA (pDNA)[22–24] and small interfering RNA (siRNA)[25]. The cytocleavable cationic

PRXs induce significantly higher gene expression of pDNA or gene silencing efficiency of siRNA than non-cleavable DMAE-PRX through the degradation of the DMAE-SS-PRXs and the efficient intracellular release of their cargos[21–25]. Thus, it is strongly anticipated that the DMAE-SS-PRXs have great potential as vehicles to achieve efficient intracellular release of active enzymes.

In this study, anionic β-galactosidase (β-gal) (464.5 kDa, pI = 4.6) was selected as a model enzyme to form a polyelectrolyte complex with the DMAE-SS-PRXs[26], and the reduction-induced reactivation of enzymes was demonstrated (**Fig. 1**). Furthermore, the intracellular delivery and intracellular enzymatic activity were evaluated in comparison with the non-cleavable DMAE-PRXs and the CPP-based commercial reagent.

Table 1 | Characterization of the polyrotaxanes used in this study

Sample code	Number of threading α-CD[a]	Number of DMAE group on PRX[b]	Number of DMAE group on α-CD[b]	M_n[c]
DMAE-SS-PRX	52 (46%)	301	5.8	94,000
DMAE-PRX	46 (41%)	264	5.7	85,000

[a]Determined by ^{1}H NMR in 0.1 M NaOD/D_2O (**Supplementary Fig. S1**). The values in parentheses represent the percentage of CD coverage on the PEG chain, assuming one CD molecule includes two repeating units of ethylene glycol. [b]Determined by ^{1}H NMR in D_2O (**Supplementary Fig. S1**). [c]Calculated based on the chemical composition determined by ^{1}H NMR.

Results

Preparation and characterization of DMAE-SS-PRX/β-gal polyelectrolyte complexes. To form a polyelectrolyte complex with the anionic β-gal, the reduction-cleavable DMAE-SS-PRXs were synthesized as summarized in **Table 1**. The DMAE-SS-PRX/β-gal complexes were prepared by mixing each solution at various N/C ratios (defined as the molar ratio of the cationic DMAE groups in the DMAE-SS-PRX to the anionic carboxylic acid residues (Asp and Glu) in β-gal). The formation of the complexes was confirmed by native agarose gel electrophoresis (**Fig. 2A**). The β-gal band disappeared at an N/C ratio of 1.5. The diameter and zeta potentials of the resulting complexes were characterized as shown in **Fig. 2B**. The zeta potential of native β-gal was strongly negative (−20 mV), whereas those of the complexes gradually shifted to positive values as the N/C ratio increased. The diameter of the complexes drastically increased to a relatively large diameter (approximately 1 μm) in the N/C ratio range of 0.5 to 3. For the N/C ratios greater than this range, the diameter of the complexes decreased to 45 nm at the N/C ratio of 10.

The enzymatic activity of the DMAE-SS-PRX/β-gal complexes prepared at various N/C ratios was determined by colorimetry using *o*-nitrophenyl-β-D-galactopyranoside (ONPG) as a substrate (**Fig. 2C**). As the N/C ratio was increased, the enzymatic activity of β-gal gradually decreased and reached a plateau (approximately 32%) over the N/C ratio of 2. Herein, the DMAE-SS-PRX/β-gal complexes (N/C 2) showed almost identical circular dichroism spectra to the native β-gal (**Fig. 2D**). To determine the kinetic parameters of this reaction, the enzymatic activity of the DMAE-SS-PRX/β-gal complexes was measured at various substrate concentrations ([S]) to make Hanes-Woolf plots (**Supplementary Fig. S2**)[27,28]. The $V_{max,app}$ of the enzymatic reaction decreased as the N/C ratio increased, whereas $K_{m,app}$ remained constant (**Supplementary Table S1**).

Reduction-induced release of β-gal from complexes. When the DMAE-SS-PRX/β-gal reacts with intracellular reductive molecules such as glutathione (GSH), the supramolecular structure of the DMAE-SS-PRX may dissociate into its constitutive molecules, resulting in the release of native enzymes to recover their activity. To confirm this hypothesis, gel electrophoresis of DMAE-SS-PRX/β-gal (N/C 2) was performed after 1 h incubation in various GSH concentrations (**Fig. 3A**). At the same time, a non-cleavable DMAE-PRX with roughly comparable number of threading CDs

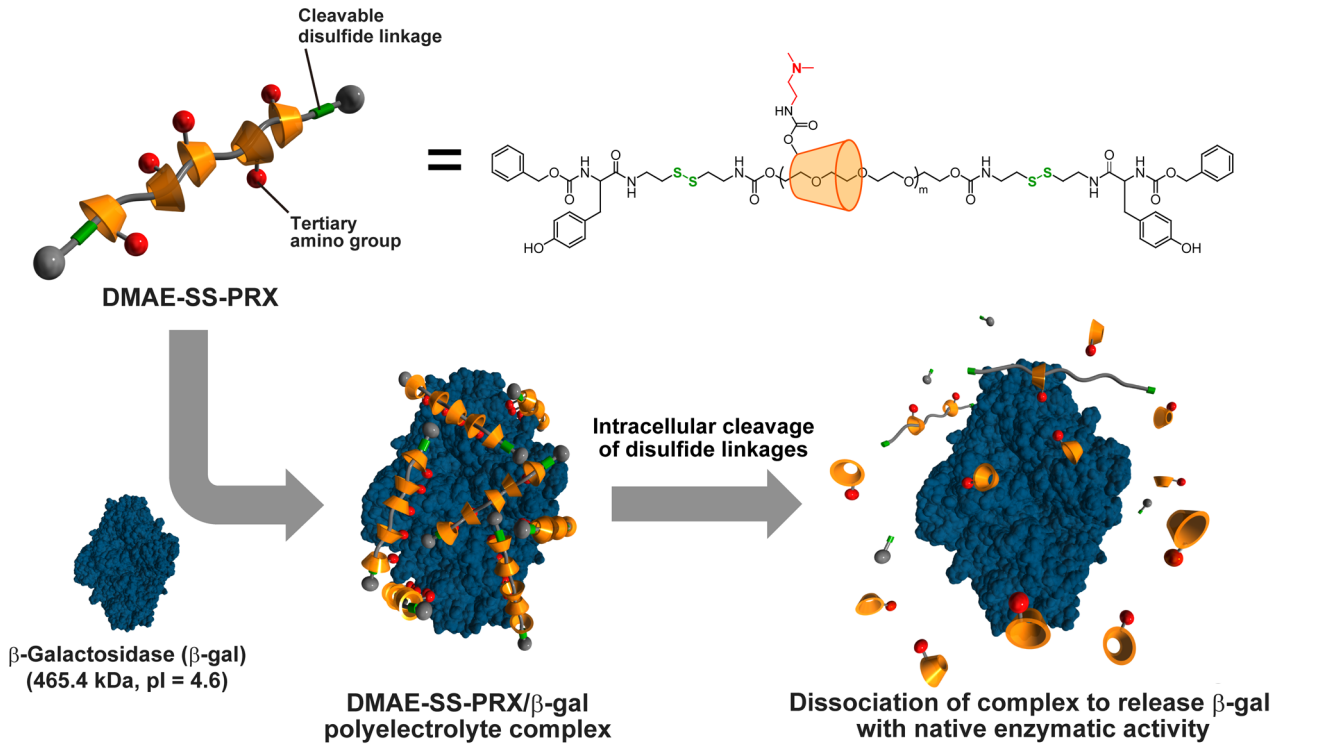

Figure 1 | Schematic illustration of the polyelectrolyte complex formation between the DMAE-SS-PRX and the anionic β-galactosidase (β-gal) and the intracellular dissociation of the complexes by the cleavage of the terminal disulfide linkages.

and DMAE groups was tested as a control (**Table 1** and **Fig. 3B**). In the case of the DMAE-SS-PRX/β-gal complexes, smeared bands of free enzyme appeared at the GSH concentrations over 1 mM, whereas no band was observed for non-cleavable DMAE-PRX/β-gal complexes, even at a GSH concentration of 5 mM. Similarly, the enzymatic activity of the cleavable DMAE-SS-PRX/β-gal and the non-cleavable DMAE-PRX/β-gal complexes (N/C 2) was determined after 1 h incubation in various concentrations of GSH (**Fig. 3C**). In the range of extracellular GSH concentrations (1 to 10 μM)[29], the enzymatic activity was almost constant (approximately 30 to 40%) for both type of PRXs. When the concentration of GSH increased to intracellular level (> 0.5 mM), the enzymatic activity of the cleavable DMAE-SS-PRX/β-gal recovered completely. Since the β-gal was released from the complexes at a high GSH concentration, the enzymatic activity is thought to be recovered. However, at the GSH concentration greater than 1 mM, the enzymatic activity decreased again, presumably due to denature of the released β-gal at a high GSH concentration (**Supplementary Fig. S4**). In contrast to the cleavable PRXs, negligible change in the enzymatic activity of the non-cleavable DMAE-PRX/β-gal was observed over the tested GSH concentration range.

Intracellular uptake and activity of the DMAE-SS-PRX/β-gal complexes. To assess the intracellular transduction ability of the DMAE-SS-PRX/β-gal complexes, confocal laser scanning microscopic (CLSM) observation of HeLa cells was performed after a 24 h incubation with samples including FITC-β-gal. As a control, a commercially available cell-penetrating peptide (CPP)-based Xfect reagent was used. To verify the intracellular localization of the FITC-β-gal (green), cell nuclei and acidic endosomes/lysosomes were stained with Hoechst 33342 (blue) and LysoTracker Red (red), respectively. As shown in **Fig. 4A**, negligible fluorescence was observed for the native FITC-β-gal. On the contrary, green spots from the FITC-β-gal were observed in the intracellular regions for Xfect, and most of the green spots were separated from the endosomes/lysosomes (**Fig. 4B**). With the PRXs, bright green signals were observed around the perinuclear regions, and they were considered to colocalize with the endosomes/lysosomes for both DMAE-SS-PRX and DMAE-PRX (**Fig. 4C and 4D**). For

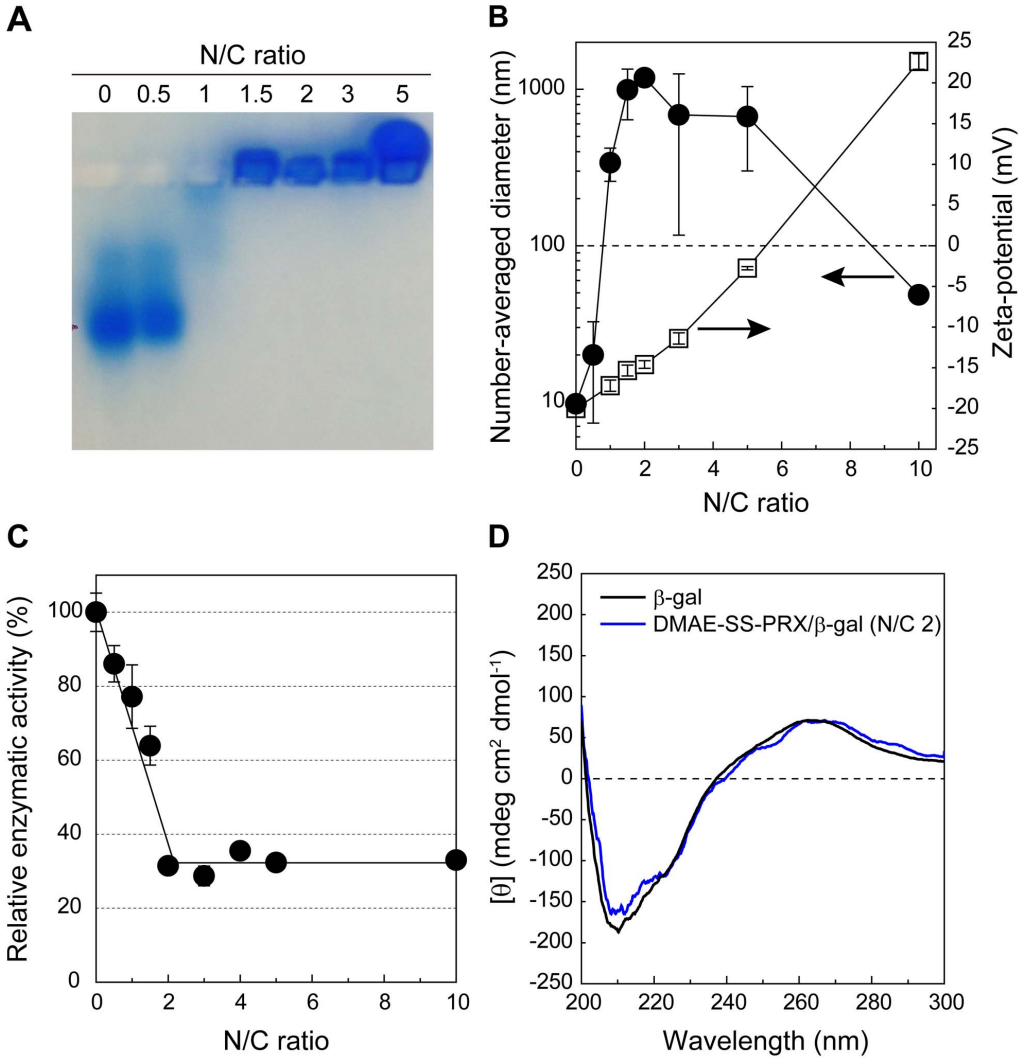

Figure 2 | Characterization of the DMAE-SS-PRX/β-gal complexes. (A) Native agarose gel electrophoresis image of the DMAE-SS-PRX/β-gal complexes at various N/C ratios. (B) Mean diameter (closed circles) and zeta potential (open squares) variations of the DMAE-SS-PRX/β-gal complexes at various N/C ratios. Data are expressed as the means ± SD of triplicate experiments. (C) Relative enzymatic activity of the DMAE-SS-PRX/β-gal complexes at various N/C ratios. Data are expressed as the means ± SD of triplicate experiments. (D) Far-UV circular dichroism spectra of free β-gal (black line) and the DMAE-SS-PRX/β-gal complex (N/C 2) (blue line).

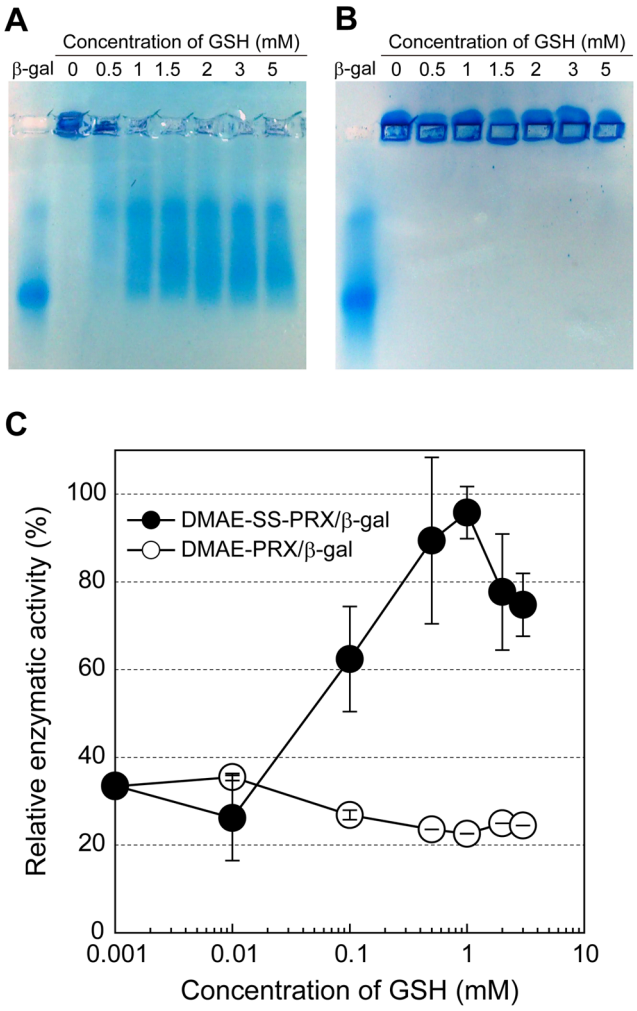

Figure 3 | Reduction-induced release of the β-gal from the complexes. (A, B) Native agarose gel electrophoresis image of cleavable DMAE-SS-PRX/β-gal (N/C 2) (A) and non-cleavable DMAE-PRX/β-gal complexes (N/C 2) (B) in the presence of various concentrations of glutathione (GSH). (C) Change in relative enzymatic activity of the cleavable DMAE-SS-PRX/β-gal (N/C 2, closed circles) and non-cleavable DMAE-PRX/β-gal complexes (N/C 2, open circles) after 1 h incubation in the presence of various concentrations of GSH. Data are expressed as the means ± SD of triplicate experiments.

quantitative comparison, the intracellular uptake level of FITC-β-gal was determined by flow cytometry (**Fig. 4E**). The intracellular uptake level of FITC-β-gal was almost the same between the cleavable DMAE-SS-PRX and the non-cleavable DMAE-PRX, and the fluorescence intensities were approximately 30-times higher than the native FITC-β-gal. Additionally, the cleavable DMAE-SS-PRX and non-cleavable DMAE-PRX showed slightly higher intracellular uptake levels of FITC-β-gal than the CPP-based Xfect reagent, even at the low N/C ratio (N/C 2).

The enzymatic activity of the DMAE-SS-PRX/β-gal complexes in living cells was evaluated using membrane-permeable TokyoGreen-β-Gal (TG-β-gal) as a fluorescent substrate[30,31]. **Fig. 5A-D** shows the CLSM images of HeLa cells after incubation with 10 μM TG-β-gal for 30 min. When the cells were treated with free β-gal, no fluorescence was observed (**Fig. 5A**). For the Xfect/β-gal and the non-cleavable DMAE-PRX/β-gal, the generation of fluorescent product was observed in both the intracellular and extracellular regions (**Fig. 5B and 5D**). The observed extracellular fluorescence may be due to the diffusion of fluorescent products (2-Me-4OMe TG) into the extracellular medium[32]. On the contrary, a remarkably bright fluorescence was observed in the intracellular region for the cleavable DMAE-SS-PRX/β-gal, indicating its superior enzymatic activity in the intracellular environment (**Fig. 5C**). To determine the fluorescence intensity and to compare the kinetics of intracellular enzymatic reaction, a time-course of the fluorescence intensity change was monitored after the addition of TG-β-gal (**Fig. 5E**). Overall, the cleavable DMAE-SS-PRX/β-gal complex-treated cells showed the largest and most persistent change in fluorescence intensity, consistent with the CLSM observation (**Fig. 5C**). The non-cleavable DMAE-PRX/β-gal was less effective in intracellular enzymatic activity compared to Xfect. The free β-gal-treated cells showed negligible change in fluorescence intensity.

Next, the effect of the N/C ratio of the DMAE-SS-PRX/β-gal complex on cellular internalization and intracellular enzymatic activity was investigated (**Supplementary Fig. S3**). The intracellular uptake level of the DMAE-SS-PRX/FITC-β-gal complex increased with the N/C ratio and reached a plateau value over an N/C ratio of 5 (**Supplementary Fig. S3**). The intracellular enzymatic activity of the DMAE-SS-PRX/β-gal complex also increased with the N/C ratio of the complex (**Supplementary Fig. S3**).

Therapeutic application of DMAE-SS-PRX/β-gal complexes for enzyme-prodrug therapy. To assess the therapeutic potential of the DMAE-SS-PRX/β-gal complexes, intracellular activation of anticancer prodrug was performed with 5-fluorouridine-5′-*O*-β-D-galactopyranoside (5-FUR-β-gal), which is a galactosylated analogue of 5-fluorouridine (5-FUR) (**Fig. 6**)[33]. The 5-FUR shows dose-dependent cytotoxicity against HeLa cells, whereas negligible cytotoxicity was observed for 5-FUR-β-gal (**Fig. 6B**). Because the galactosyl residue of 5-FUR-β-gal is hydrolyzed by β-galactosidase and converted into cytotoxic 5-FUR[33], intracellular enzymatic activation of 5-FUR-β-gal in the presence of the DMAE-SS-PRX/β-gal complex was tested by a cell viability assay (**Fig. 6C**). Without the 5-FUR-β-gal treatment, the DMAE-SS-PRX/β-gal complex (N/C 2) treated cells were viable at a β-gal concentration range of 10 to 100 nM, indicating low cytotoxicity of the DMAE-SS-PRX/β-gal complex. Additionally, without the treatment of the DMAE-SS-PRX/β-gal complex, the 5-FUR-β-gal-treated cells showed negligible cytotoxicity. In sharp contrast, the successive treatment of the DMAE-SS-PRX/β-gal complex and the 5-FUR-β-gal caused a marked cytotoxicity in a β-gal concentration-dependent manner. At the β-gal concentration of 100 nM, the relative cell viability was almost comparable to the 5-FUR-treated cells. In the presence of the 5-FUR-β-gal, cellular viability of the non-cleavable DMAE-PRX/β-gal and the Xfect/β-gal remained high compared to the cleavable DMAE-SS-PRX/β-gal.

Discussion

Our strategy to activate the therapeutic enzymes delivered in cells includes; (1) intracellular uptake of the enzyme using cleavable PRXs, (2) degradation of the PRXs by the cleavage of the terminal cleavable linkages, and (3) release of the enzymes and the subsequent reactivation of the enzymatic activity (**Fig. 1**). In this study, β-gal was selected as a model enzyme because of its potential in clinical application for enzyme-prodrug therapy and enzyme replacement therapy[3,4]. As seen in **Fig. 2A**, the β-gal and the DMAE-SS-PRX formed a polyelectrolyte complex upon mixing with an appropriate N/C ratio. At the N/C ratio range of 1 to 5, the DMAE-SS-PRX/β-gal complexes had large diameters and low zeta-potential values, most likely due to the weak electrostatic repulsive force between the complexes through charge neutralization (**Fig. 2B**). Over the N/C ratio of 5, the diameter of the complexes decreased. This result suggests that the aggregation of the complexes is prohibited due to their strongly positive charge.

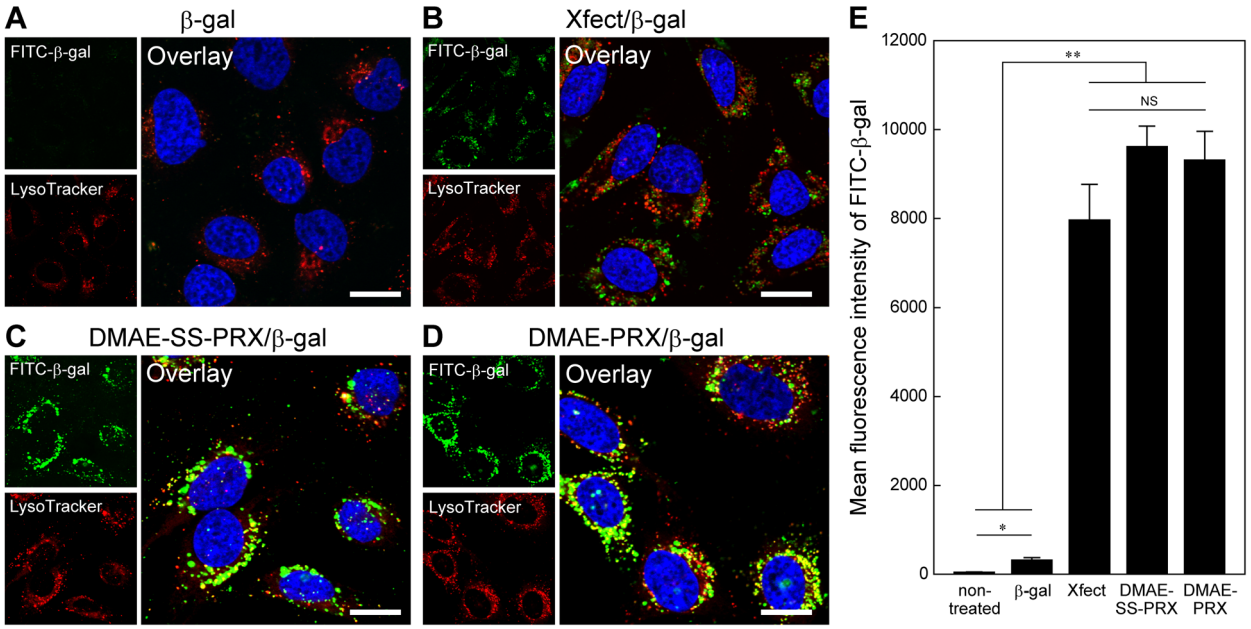

Figure 4 | Cellular internalization of the DMAE-SS-PRX/β-gal complexes. (A-D) CLSM images of HeLa cells after 24 h incubation with FITC-β-gal (A) cell-penetrating peptide-based Xfect/FITC-β-gal (B) cleavable DMAE-SS-PRX/FITC-β-gal (N/C 2) (C) and non-cleavable DMAE-PRX/FITC-β-gal (N/C 2) (D) (scale bars: 20 μm). The nuclei and the late endosomes/lysosomes were visualized with Hoechst 33342 (blue) and LysoTracker Red (red), respectively. (E) Mean fluorescence intensities of HeLa cells after 24 h incubation with FITC-β-gal, Xfect/FITC-β-gal, cleavable DMAE-SS-PRX/FITC-β-gal (N/C 2), and non-cleavable DMAE-PRX/FITC-β-gal (N/C 2) as determined by flow cytometry. In these experiments, the initial concentration of FITC-β-gal in the medium was adjusted to 20 nM. Data are expressed as the means ± SD of triplicate experiments (*$p < 0.05$, **$p < 0.001$, NS indicates not significant).

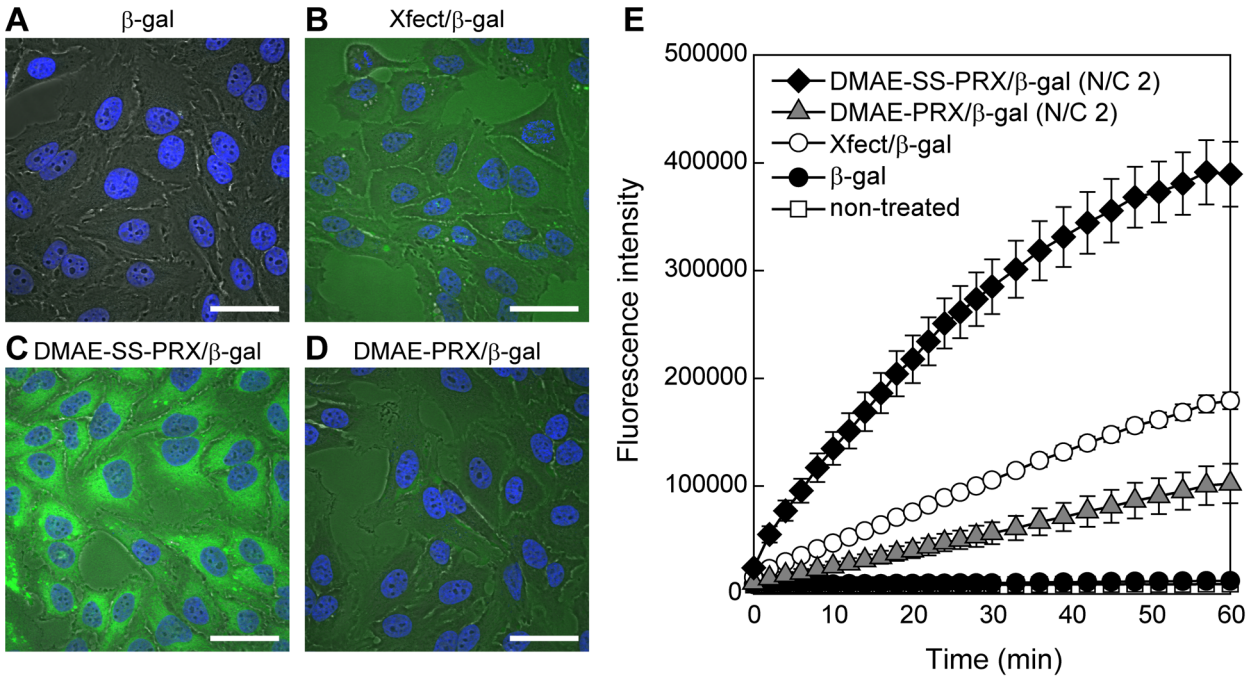

Figure 5 | Enzymatic activity of the β-gal delivered into the cells. (A-D) CLSM images of HeLa cells after 24 h incubation with β-gal (A), cell-penetrating peptide-based Xfect/β-gal (B), cleavable DMAE-SS-PRX/β-gal (N/C 2) (C), and non-cleavable DMAE-PRX/β-gal (N/C 2) (D), followed by 30 min incubation after addition of TG-β-gal as a fluorescent substrate (scale bars: 50 μm). (E) Time-course of the fluorescence intensity change of TG-β-gal in HeLa cells after 24 h incubation with β-gal (closed circles), Xfect/β-gal (open circles), cleavable DMAE-SS-PRX/β-gal (N/C 2) (closed diamonds), non-cleavable DMAE-PRX/β-gal (N/C 2) (closed triangles), and non-treated (open squares). The initial concentration of β-gal in the medium was adjusted to 20 nM. Data are expressed as the means ± SD of triplicate experiments.

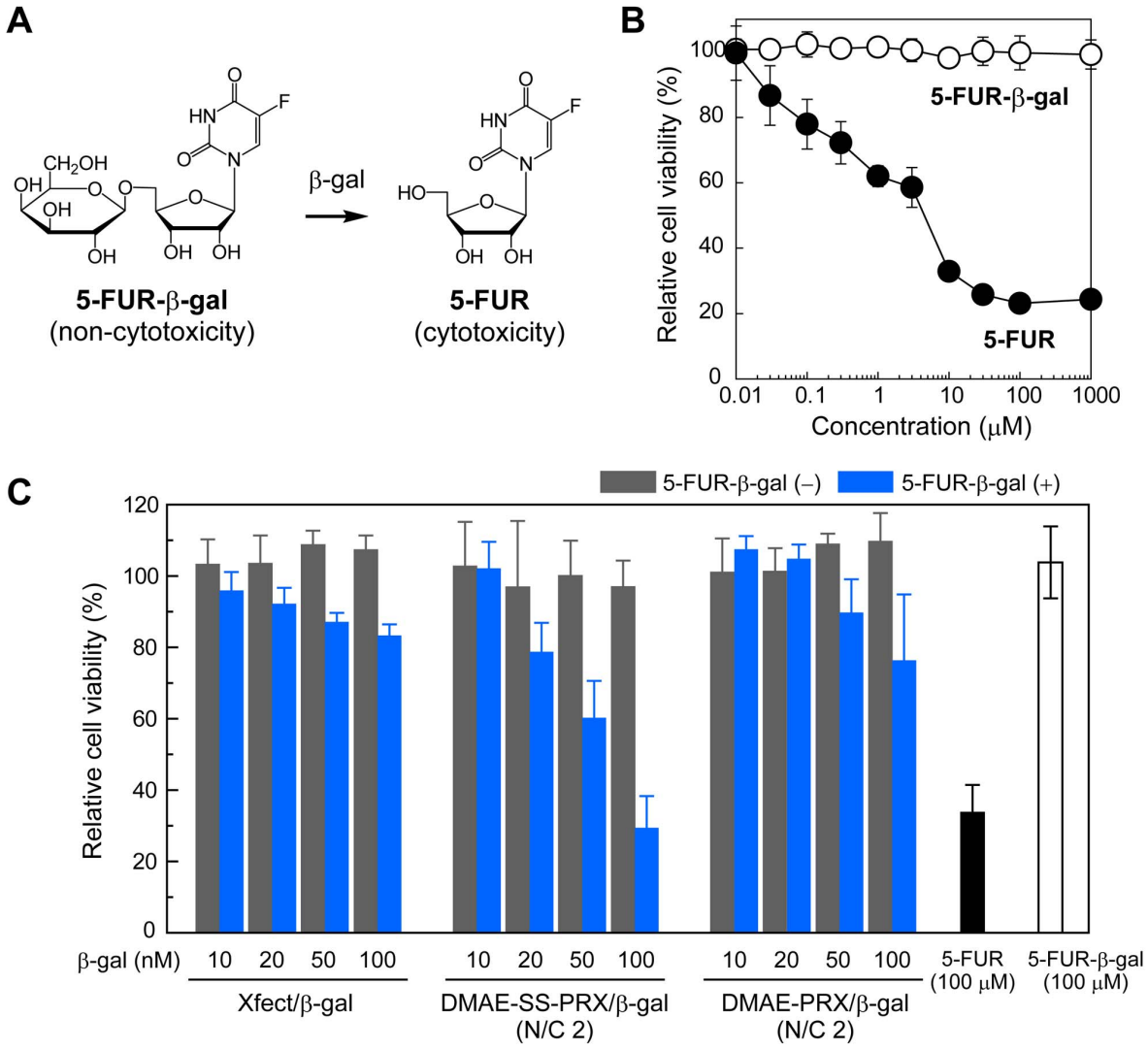

Figure 6 | Activation of anticancer prodrugs by the DMAE-SS-PRX/β-gal complexes. (A) Chemical structures of 5-fluorouridine-5′-*O*-β-D-galactopyranoside (5-FUR-β-gal) and 5-fluorouridine (5-FUR). (B) Relative viability of HeLa cells incubated for 24 h with 5-FUR-β-gal (open circles) and 5-FUR (closed circles). (C) Relative viability of HeLa cells treated with Xfect/β-gal, cleavable DMAE-SS-PRX/β-gal complexes (N/C 2), and non-cleavable DMAE-PRX/β-gal complexes (N/C 2) at various β-gal concentrations for 24 h, followed by incubation with or without 5-FUR-β-gal (100 μM) for 24 h. Data are expressed as the means ± SD (n = 6).

When the β-gal forms a polyelectrolyte complex with cationic polymers or nanoparticles, its enzymatic activity often disappears, most likely due to the masking of the active site of the enzymes[16,17]. Because the active site of β-gal is an anionic Glu residue, the activity of β-gal decreases through the masking of the anionic active site through electrostatic interactions[34,35]. However, the kinetics study revealed that the DMAE-SS-PRX acts as a non-competitive inhibitor for β-gal (**Supplementary Fig. S2**). This means that the DMAE-SS-PRX binds to the neighboring anionic amino acid residues of the active site and reduces the catalytic reaction rate while maintaining the binding constant of the substrate[27,28,36]. The enzymatic activity of the DMAE-SS-PRX/β-gal complexes was not completely inhibited and still remained at 32% of activity, even at high N/C ratios (**Fig. 2C**). In the case of the polyelectrolyte complex between β-gal and cationic polymers such as poly(*N*,*N*-diethylaminoethyl methacrylate) or poly(allylamine), the enzymatic activity of β-gal is reported to be completely inhibited[37]. Therefore, the DMAE-SS-PRX is considered to loosely associate with β-gal to allow the access of a substrate to some extent. In the case of the polyelectrolyte complex of the DMAE-SS-PRX with nucleic acids, the DMAE-SS-PRXs form a loosely associated complex with pDNA or siRNA, as revealed by a dye exclusion assay[23,25]. Taking this fact into account, it is hypothesized that the supramolecular framework of PRXs is a potentially valid and feasible way to form complexes with enzymes without denaturation. Indeed, the β-gal retained its native three dimensional structure throughout the complexation with the DMAE-SS-PRXs (**Fig. 2D**). Additionally, the freely mobile nature of threaded CDs in the DMAE-SS-PRX enhances the multivalent electrostatic interaction with anionic enzymes through the improvement of spatial mismatch in the interaction[22]. Therefore, the DMAE-SS-PRX/β-gal complexes are thought to be sufficiently stable for the intracellular delivery.

As shown in **Fig. 3C**, the activity of the DMAE-SS-PRX/β-gal complexes was recovered upon the addition of GSH, especially at intracellular concentrations (> 0.5 mM)[29]. This result is due to the cleavage of the terminal disulfide linkages of DMAE-SS-PRX and the subsequent release of enzymes, as confirmed by gel electrophoresis (**Fig. 3A**). The bands of the released β-gal were smeared, most likely due to the incomplete dissociation of the complexes and/or the inclusion of the hydrophobic amino acid into the cavity of the dethreaded CDs. In contrast to the cleavable DMAE-SS-PRX/β-gal complexes, the non-cleavable DMAE-PRX/β-gal complexes did not release β-gal

upon the addition of GSH, resulting in negligible recovery of enzymatic activity (**Fig. 3B and 3C**). This fact strongly supports our hypothesis that the GSH-induced release of β-gal is attributable to the recovery of enzymatic activity of the DMAE-SS-PRX/β-gal complexes. At the GSH concentrations greater than 1 mM, the enzymatic activity of the DMAE-SS-PRX/β-gal complexes decreased. This is most likely due to the denaturing of the enzyme by the reaction with high concentrations of GSH. Indeed, the activity of the native β-gal decreased in a GSH concentration-dependent manner (**Supplementary Fig. S4**).

The intracellular uptake is of significant importance for inducing the function of exogenous enzymes in cells. Flow cytometric measurements revealed that the DMAE-SS-PRX showed comparable cellular uptake to the CPP-based Xfect (**Fig. 4E**). Although the intracellular uptake level of the DMAE-SS-PRX/β-gal complexes increased with the N/C ratio (**Supplementary Fig. S3**), the N/C ratio of 2 was selected for the cellular experiment to avoid the potential toxic effect derived from excess DMAE-SS-PRX[38,39]. To confirm the intracellular distribution of delivered β-gal, the CLSM observation was performed. It is revealed that the intracellular localizations of the DMAE-SS-PRX/β-gal complexes and the Xfect/β-gal complexes were completely different, presumably due to a difference in the cellular uptake pathway (**Fig. 4B and 4C**). The Xfect internalizes into cells through macropinocytosis or caveolae-mediated endocytosis[40]. Therefore, Xfect/β-gal is observed as separated from acidic lysosomes because macropinosomes are leaky vesicles, and caveosomes are not involved in the reduction of pH[41]. On the contrary, the DMAE-SS-PRX/β-gal colocalized with the acidic lysosomes, indicating that the DMAE-SS-PRX/β-gal entered into the cells through a different pathway, such as clathrin-mediated endocytosis[42]. There was a negligible difference in the cellular uptake level and intracellular localization between the cleavable DMAE-SS-PRX and the non-cleavable DMAE-PRX (**Fig. 4C, 4D, and 4E**), indicating that the terminal linker did not affect the cellular internalization of the complexes.

Herein, the diameter of the DMAE-SS-PRX/β-gal complex at the N/C 2 seems too large for cellular internalization (1 μm). In our CLSM observation, the diameter of the DMAE-SS-PRX/FITC-β-gal determined from a pixel in the images was actually smaller than the diamter determined by DLS. Taking this fact into account, two possible reasons arise to explain intercellular trafficking of the complex prepared at the N/C ratio of 2: the dissociation of the complexes in the medium, and over estimation of the diameter by DLS. Since the polyelectrolyte complexes are known to dissociate in the culture medium by simple dilution or interaction with serum proteins[25], it is plausible that the dissociated complexes are to be internalized into cells. Additionally, since the light scattering intensity is increased with the size, larger particles are detected more sensitive than smaller ones in DLS measurements, which can lead to over estimation of the size. In any cases, it seems obvious that the small particle fraction of the complexes is thought to internalize dominantly into cells. The negative surface charge is also a negative impact in cellular internalization. Although the zeta potential value of the DMAE-SS-PRX/β-gal prepared at the N/C 2 is approximately −15 mV, the cellular internalization of the complexes was clearly observed (**Fig. 4C**). In the process of cellular internalization, the complexes are first allowed to interact with the surface of the cells, followed by internalized into cells through endocytosis machinery. Thus, it seems that the positively charged particles are allowed to interact more effectively with negatively charged cellular membrane than the neutral or negatively charged particles. However, the cellular internalization of the anionic polyelectrolyte complexes was also observed in various reports[43,44]. This fact indicates that the anionic complexes are allowed to interact with the receptor proteins on the cellular membrane and involve the endocytosis. Therefore, the DMAE-SS-PRX/β-gal complexes are thought to internalize into cells even at low N/C ratio.

The intracellular activity of the cleavable DMAE-SS-PRX/β-gal was markedly higher than the non-cleavable DMAE-PRX/β-gal activity (**Fig. 5C, 5D, and 5E**). This result suggests that DMAE-SS-PRX/β-gal dissociated to release β-gal by intracellular cleavage of DMAE-SS-PRX[22]. The non-cleavable DMAE-PRX/β-gal complexes were retained in the complex form, and their activity was inhibited. The intracellular enzymatic activity of the Xfect/β-gal was also lower than the DMAE-SS-PRX/β-gal activity, despite the comparable cellular uptake levels of the enzyme and a difference in the cellular uptake pathway. To assess this result, the enzymatic activity of Xfect/β-gal was demonstrated using ONPG as a substrate (**Supplementary Fig. 5**). The enzymatic activity of Xfect/β-gal completely diminished and negligible recovery of the activity was observed upon the addition of GSH. To further evaluate the intracellular activity of the delivered enzymes, the enzyme-prodrug assay was performed using 5-FUR-β-gal as an anticancer prodrug (**Fig. 6**)[33]. At a β-gal concentration of 100 nM, the viability of the DMAE-SS-PRX/β-gal and the 5-FUR-β-gal-treated cells was the same as the 5-FUR-treated cells, indicating that most of the 5-FUR-β-gal was converted into cytotoxic 5-FUR in the intracellular environment. Because the intracellular enzymatic activity of the non-cleavable DMAE-PRX/β-gal and the Xfect/β-gal was significantly lower than the DMAE-SS-PRX/β-gal (**Fig. 5**), the DMAE-SS-PRX/β-gal was thought to show the highest anticancer effect.

In summary, the intracellular delivery of enzymes and the subsequent intracellular reactivation of the enzyme were achieved by a polyelectrolyte complex formation with cytocleavable DMAE-SS-PRXs. The intracellularly cleavable DMAE-SS-PRXs provide an attractive technique for delivering therapeutic enzymes into living cells and reactivating the enzymes in response to the intracellular environment.

Methods

Reagents. Poly(ethylene glycol) (PEG) (M_n = 9,810, M_w/M_n = 1.02) (Sigma-Aldrich, St. Louis, MO, USA) was used for the synthesis of PRX. The cytocleavable DMAE-SS-PRX and the non-cleavable DMAE-PRX were synthesized as previously reported[22–25]. The number of threading α-CDs and the number of modified DMAE groups on the PRXs were determined by ^{1}H NMR spectra (**Supplementary Fig. S1**) and the characterization of the PRXs was summarized in **Table 1**. β-Galactosidase from *Escherichia coli* (β-gal) (EC 3.2.1.23), L-glutathione (GSH), and *o*-nitrophenyl-β-D-galactopyranoside (ONPG) were obtained from Sigma-Aldrich. Fluorescein isothiocyanate-labeled β-galactosidase (FITC-β-gal) was prepared as previously reported[45]. Xfect protein transfection reagent, a cell penetrating peptide-based protein carrier, was obtained from Clontech (Mountain View, CA, USA) and was used according to the manufacturer's instruction. 5-Fluorouridine-5′-*O*-β-D-galactopyranoside (5-FUR-β-gal) and 5-fluorouridine (5-FUR) were obtained from Carbosynth (Berkshire, UK) and TCI (Tokyo, Japan), respectively.

Preparation and characterization of the DMAE-SS-PRX/β-gal complexes. The β-gal was dissolved in 10 mM HEPES buffer (pH 7.4) to prepare a 15 μM stock solution. To this solution, the DMAE-SS-PRXs solution was added at various N/C ratios (molar ratio of the cationic DMAE groups of the DMAE-SS-PRX to the anionic Asp and Glu residues of β-gal) and allowed to sit for 1 h to form the polyelectrolyte complexes (final concentration of β-gal: 2.5 μM). The formation of the DMAE-SS-PRX/β-gal complex was confirmed by native agarose gel electrophoresis. The complex solutions (20 μL) were mixed with BlueJuice gel loading buffer (Invitrogen) (1 μL), and 15 μL of the solutions was applied to 0.8% agarose gel (Sigma-Aldrich). The electrophoresis was performed in TBE buffer (44.5 mM tris, 44.5 mM boronic acid, and 1 mM EDTA) for 20 min at 200 V. The gel was placed in CBB staining solution (0.2% CBB R-250, 10% acetic acid, and 45% methanol) for 10 min, followed by incubation in destaining solution (10% acetic acid and 25% methanol). Similarly, gel electrophoresis of the DMAE-SS-PRX/β-gal and the DMAE-PRX/β-gal complexes (N/C 2) in the presence of GSH was conducted. To the complex solutions, GSH was added at various concentrations and incubated for 1 h. The electrophoresis was performed as described above.

Circular dichroism spectra were recorded on a J-725 spectropolarimeter (Jasco, Tokyo, Japan) at 25°C. The diameter and the zeta potential of the DMAE-SS-PRX/β-gal complexes were determined on a Zetasizer Nano ZS (Malvern Instruments, Malvern, UK) equipped with a 4 mW He–Ne laser (633 nm). The dynamic light scattering (DLS) measurements were conducted at 25°C at a detection angle of 173°. The obtained autocorrelation functions were analyzed by the CONTIN method to determine number-averaged diameters. The electrophoretic light scattering measurements were performed at 25°C.

Enzymatic activity assay. DMAE-SS-PRX/β-gal complexes with various N/C ratios were prepared in a 10 mM HEPES buffer solution (pH 7.4) at a β-gal concentration of 20 nM. The substrate solution (10 mM ONPG in 10 mM HEPES buffer) (225 μL) was added to an equal volume of the DMAE-SS-PRX/β-gal complexes and the β-gal solutions, and a time-course of the increment in absorbance at 410 nm was recorded on a V-550 UV-VIS spectrophotometer (Jasco) for 1 min. The relative enzymatic activity was determined from the initial slope of the absorbance variation derived from the product. Similarly, the enzymatic activity of the DMAE-SS-PRX/β-gal and the DMAE-PRX/β-gal complexes (N/C 2) in the presence of GSH was determined. To the complex solutions, GSH was added at various concentrations. After incubation for 1 h, the enzymatic activity was determined as described above.

Intracellular uptake analysis by flow cytometry. HeLa cells derived from human cervical carcinoma were obtained from the Japanese Collection of Research Bioresources (JCRB, Osaka, Japan) and grown in minimum essential medium (MEM) (Gibco BRL, Grand Island, NY, USA) containing 10% fetal bovine serum (FBS) (Gibco), 100 units/mL penicillin, and 100 μg/mL streptomycin (Gibco) in a humidified 5% CO_2 atmosphere at 37°C. HeLa cells were seeded on a 24-well plate (BD Falcon, Franklin Lakes, NJ, USA) at a density of 5×10^4 cells/cm^2 and incubated overnight. After the medium was exchanged with fresh medium (270 μL), the sample solutions (30 μL) were applied to each well (final concentration of FITC-β-gal: 20 nM). After incubation for 24 h, the cells were washed three times with phosphate buffered saline (PBS) and harvested by treatment with 0.25% trypsin (Gibco). The cells were collected by centrifugation (1,000 rpm, 4°C, 5 min) and suspended in PBS containing 0.1% bovine serum albumin (BSA) (Sigma-Aldrich) (400 μL). After the cells were passed through a 35 μm cell strainer (BD Falcon), flow cytometry measurements were performed on a FACSCanto II (BD Biosciences). The FITC-β-gal was excited with 20 mW solid-state laser (488 nm) and detected with a 515–545 nm bandpass filter. In total, 10,000 cells were acquired for each sample and the mean fluorescence intensity of the cell population was analyzed by DIVA software (BD Biosciences).

Confocal laser scanning microscopic (CLSM) observation. HeLa cells were seeded on 35-mm glass-bottom dishes (Iwaki, Tokyo, Japan) at a density of 1×10^4 cells/cm^2 and incubated overnight. After the medium was exchanged with fresh MEM (900 μL), the sample solutions (100 μL) were applied to the dish (final concentration of FITC-β-gal: 20 nM). After incubation for 24 h, the cells were washed twice with PBS and stained with LysoTracker Red DND-99 (Molecular Probes, Eugene OR, USA) (500 nM) for 60 min at 37°C, followed by staining with Hoechst 33342 (Dojindo Laboratories) (1 μg/mL) for 10 min at 37°C. The CLSM observations were performed on a FluoView FV10i (Olympus, Tokyo, Japan) equipped with a 60 × water-immersion objective lens (N/A 1.2) and a diode laser. The excitation wavelength was 405 nm (17.1 mW) for Hoechst 33342, 473 nm (11.9 mW) for FITC-β-gal, and 559 nm (15 mW) for LysoTracker Red.

Similarly, the intracellular enzymatic activities of the complexes were observed with Tokyo Green-β-Gal (TG-β-gal) (Sekisui Medical, Tokyo, Japan) as a fluorescent substrate. TG-β-gal (10 μM) was added to the dish and the cells were incubated for 30 min at 37°C. The CLSM observations were performed on a FluoView FV10i at an excitation wavelength of 473 nm.

Enzymatic activity assay in living cells. HeLa cells were seeded on a 24-well plate at a density of 5×10^4 cells/cm^2 and incubated overnight. After the medium was exchanged with fresh medium (270 μL), the sample solutions (30 μL) were applied to each well (final concentration of β-gal: 20 nM). After incubation for 24 h, the cells were washed three times with PBS. After the addition of TG-β-gal (10 μM), the change in fluorescence intensity was recorded on an ARVO MX multilabel counter (Perkin Elmer, Wellesley, MA, USA) using an appropriate filter set (excitation: 485/14 nm, emission: 535/25 nm).

Enzyme-prodrug assay with 5-fluorouridine-5′-*O*-β-D-galactopyranoside. HeLa cells were seeded on a 96-well plate (BD Falcon) at a density of 2.5×10^4 cells/cm^2 and incubated overnight. After the medium was exchanged with fresh MEM (90 μL), the DMAE-SS-PRX/β-gal complex solutions (10 μL) (N/C 2) were applied to each well. After incubation for 24 h, the cells were washed three times with PBS and 5-FUR-β-gal (100 μM) was added to each well. After further incubation for 24 h, Cell Counting Kit-8 reagent (Dojindo Laboratories) (10 μL) was added to each well and incubated for 1 h at 37°C. The absorbance at 450 nm was measured on a Multiskan FC plate reader (Thermo Fisher Scientific, Waltham, MA, USA). The cellular viability was calculated relative to the non-treated cells.

Statistical analysis. Data were analyzed by one-way ANOVA followed by Turkey's multiple comparison test. A *p*-value of less than 0.05 was considered to indicate statistical significance. The values are expressed as the mean ± standard deviation (S.D.).

1. Leader, B., Baca, Q. J. & Golan, D. E. Protein therapeutics: a summary and pharmacological classification. *Nat. Rev. Drug Discov.* **7**, 21–39 (2008).
2. Vlieghe, P., Lisowski, V., Martinez, J. & Khrestchatisky, M. Synthetic therapeutic peptides: science and market. *Drug Discov. Today* **15**, 40–56 (2010).
3. Brady, R. O. & Schiffmann, R. Enzyme-replacement therapy for metabolic storage disorders. *Lancet Neurol.* **3**, 752–756 (2004).
4. Rooseboom, M., Commandeur, J. N. & Vermeulen, N. P. Enzyme-catalyzed activation of anticancer prodrugs. *Pharmacol. Rev.* **56**, 53–102 (2004).
5. Toro, A. & Grunebaum, E. TAT-mediated intracellular delivery of purine nucleoside phosphorylase corrects its deficiency in mice. *J. Clin. Invest.* **116**, 2717–2726 (2006).
6. Schwarze, S. R., Ho, A., Vocero-Akbani, A. & Dowdy, S. F. In vivo protein transduction: delivery of a biologically active protein into the mouse. *Science* **285**, 1569–1572 (1999).
7. Wadia, J. S. & Dowdy, S. F. Transmembrane delivery of protein and peptide drugs by TAT-mediated transduction in the treatment of cancer. *Adv. Drug Deliv. Rev.* **57**, 579–596 (2005).
8. Gu, Z., Biswas, A., Zhao, M. & Tang, Y. Tailoring nanocarriers for intracellular protein delivery. *Chem. Soc. Rev.* **40**, 3638–3655 (2011).
9. Nochi, T. *et al.* Nanogel antigenic protein-delivery system for adjuvant-free intranasal vaccines. *Nat. Mater.* **9**, 572–578 (2010).
10. Yan, M. *et al.* A novel intracellular protein delivery platform based on single-protein nanocapsules. *Nat. Nanotechnol.* **5**, 48–53 (2010).
11. van Dongen, S. F. *et al.* Cellular integration of an enzyme-loaded polymersome nanoreactor. *Angew. Chem. Int. Ed.* **49**, 7213–7216 (2010).
12. Fischer, N. O., McIntosh, C. M., Simard, J. M. & Rotello, V. M. Inhibition of chymotrypsin through surface binding using nanoparticle-based receptors. *Proc. Natl. Acad. Sci. USA.* **99**, 5018–5023 (2002).
13. Lee, Y. *et al.* A protein nanocarrier from charge-conversion polymer in response to endosomal pH. *J. Am. Chem. Soc.* **129**, 5362–5363 (2007).
14. Harada, A. & Kataoka, K. Switching by pulse electric field of the elevated enzymatic reaction in the core of polyion complex micelles. *J. Am. Chem. Soc.* **125**, 15306–15307 (2003).
15. Harada, A. & Kataoka, K. On-off control of enzymatic activity synchronizing with reversible formation of supramolecular assembly from enzyme and charged block copolymers. *J. Am. Chem. Soc.* **121**, 9241–9242 (1999).
16. Wenck, K., Koch, S., Renner, C., Sun, W. & Schrader, T. A noncovalent switch for lysozyme. *J. Am. Chem. Soc.* **129**, 16015–16019 (2007).
17. Tomita, S. *et al.* Enzyme switch by complementary polymer pair system (CPPS). *Soft Matter* **6**, 5320–5326 (2010).
18. Akiyoshi, K., Sasaki, Y. & Sunamoto, J. Molecular chaperone-like activity of hydrogel nanoparticles of hydrophobized pullulan: thermal stabilization with refolding of carbonic anhydrase B. *Bioconjugate Chem.* **10**, 321–324 (1999).
19. Wenz, G., Han, B. H. & Müller, A. Cyclodextrin rotaxanes and polyrotaxanes. *Chem. Rev.* **106**, 782–817 (2006).
20. Li, J. & Loh, X. J. Cyclodextrin-based supramolecular architectures: syntheses, structures, and applications for drug and gene delivery. *Adv. Drug Deliv. Rev.* **60**, 1000–1017 (2008).
21. Yui, N., Katoono, R. & Yamashita, A. Functional cyclodextrin polyrotaxanes for drug delivery. *Adv. Polym. Sci.* **222**, 55–77 (2009).
22. Ooya, T. *et al.* Biocleavable polyrotaxane-plasmid DNA polyplex for enhanced gene delivery. *J. Am. Chem. Soc.* **128**, 3852–3853 (2006).
23. Yamashita, A. *et al.* Synthesis of a biocleavable polyrotaxane-plasmid DNA (pDNA) polyplex and its use for the rapid nonviral delivery of pDNA to cell nuclei. *Nat. Protoc.* **1**, 2861–2869 (2006).
24. Yamashita, A. *et al.* Supramolecular control of polyplex dissociation and cell transfection: efficacy of amino groups and threading cyclodextrins in biocleavable polyrotaxanes. *J. Control. Release* **131**, 137–144 (2008).
25. Tamura, A. & Yui, N. Cellular internalization and gene silencing of siRNA polyplexes by cytocleavable cationic polyrotaxanes with tailored rigid backbones. *Biomaterials* **34**, 2480–2491 (2013).
26. Boyer, P. D. *The Enzymes* (Academic Press, New York, 1972).
27. Copeland, R. A. *Enzymes:a practical introduction to structure, mechanism, and data analysis* (John Wiley & Sons, New York, 2004).
28. Marangoni, A. G. *Enzymatic kinetics:a modern approach* (John Wiley & Sons, New York, 2003).
29. Meister, A. & Anderson, M. E. Glutathioine. *Ann. Rev. Biochem.* **52**, 711–760 (1983).
30. Urano, Y. *et al.* Evolution of fluorescein as a platform for finely tunable fluorescence probes. *J. Am. Chem. Soc.* **127**, 4888–4894 (2005).
31. Ayame, H., Morimoto, N. & Akiyoshi, K. Self-assembled cationic nanogels for intracellular protein delivery. *Bioconjug. Chem.* **19**, 882–890 (2008).
32. Kamiya, M. *et al.* An enzymatically activated fluorescence probe for targeted tumor imaging. *J. Am. Chem. Soc.* **129**, 3918–3929 (2007).
33. Abraham, R. *et al.* Conjugates of COL-1 monoclonal antibody and β-D-galactosidase can specifically kill tumor cells by generation of 5-fluorouridine from the prodrug β-D-galactosyl-5-fluorouridine. *Cell Biophys.* **24**, 127–133 (1994).
34. Yuan, J., Martinez-Bilbao, M. & Huber, R. E. Substitutions for Glu-537 of β-galactosidase from Escherichia coli cause large decreases in catalytic activity. *Biochem. J.* **299**, 527–531 (1994).
35. Verma, A., Simard, J. M., Worrall, J. W. & Rotello, V. M. Tunable reactivation of nanoparticle-inhibited β-galactosidase by glutathione at intracellular concentrations. *J. Am. Chem. Soc.* **126**, 13987–13991 (2004).
36. Tomita, S. & Shiraki, K. Poly(acrylic acid) is a common non-competitive inhibitor for cationic enzymes with high affinity and reversibility. *J. Polym. Sci. Part A: Polym. Chem.* **49**, 3835–3841 (2011).

37. Kurinomaru, T. *et al.* Improved complementary polymer pair system: switching for enzyme activity by PEGylated polymers. *Langmuir* **28**, 4334–4338 (2012).
38. Fischer, D., Li, Y., Ahlemeyer, B., Krieglstein, J. & Kissel, T. In vitro cytotoxicity testing of polycations: influence of polymer structure on cell viability and hemolysis. *Biomaterials* **24**, 4421–1131 (2003).
39. Boeckle, S. *et al.* Purification of polyethylenimine polyplexes highlights the role of free polycations in gene transfer. *J. Gene Med.* **6**, 1102–1111 (2004).
40. Oba, M. & Tanaka, M. Intracellular internalization mechanism of protein transfection reagents. *Biol. Pharm. Bull.* **35**, 1064–1068 (2012).
41. Khalil, I. A., Kogure, K., Akita, H. & Harashima, H. Uptake pathways and subsequent intracellular trafficking in nonviral gene delivery. *Pharmacol. Rev.* **58**, 32–45 (2006).
42. Conner, S. D. & Schmid, S. L. Regulated portals of entry into the cell. *Nature* **422**, 37–44 (2003).
43. Lee, Y. *et al.* Charge-conversion ternary polyplex with endosome disruption moiety: a technique for efficient and safe gene delivery. *Angew. Chem. Int. Ed. Engl.* **47**, 5163–5166 (2008).
44. Trubetskoy, V. S. *et al.* Recharging cationic DNA complexes with highly charged polyanions for in vitro and in vivo gene delivery. *Gene Ther.* **10**, 261–271 (2003).
45. Ghosh, P. *et al.* Intracellular delivery of a membrane-impermeable enzyme in active form using functionalized gold nanoparticles. *J. Am. Chem. Soc.* **132**, 2642–2645 (2010).

Acknowledgements

This work was financially supported by the Grant-in-Aid for Scientific Research (No. 23107004) on Innovative Areas "Nanomedicine Molecular Science" (No. 2306) from the Ministry of Education, Culture, Sports, Science, and Technology (MEXT) of Japan. We are grateful to Dr. Yuji Tsuchido for his technical assistance.

Author contributions

A.T., J.S., K.T., H.Y., Y.S., K.A. and N.Y. were involved in the design of experiments. A.T. and G.I. performed the experiments and analyzed results. K.T. and H.Y. helped in circular dichroism measurements. J.S., Y.S. and K.A. helped in enzymatic activity measurements. A.T. and N.Y. wrote the manuscript. N.Y. supervised the project. All authors discussed the results and commented on the manuscript.

Additional information

Supplementary information accompanies this paper at http://www.nature.com/scientificreports

Competing financial interests: The authors declare no competing financial interests.

How to cite this article: Tamura, A. *et al.* Molecular logistics using cytocleavable polyrotaxanes for the reactivation of enzymes delivered in living cells. *Sci. Rep.* **3**, 2252; DOI:10.1038/srep02252 (2013).